Analysis of a one-dimensional fracture model

1993 J. Phys. A: Math. Gen. 26 4521

(http://iopscience.iop.org/0305-4470/26/18/019)

J. Phys. A: Math. Gen. 26 (1993) 4521–4537. Printed in the UK

Analysis of a one-dimensional fracture model

O Morgenstern, I M Sokolov† and A Blumen

Theoretische Polymerphysik, Universität Freiburg Rheinstrasse 12, D-79104 Freiburg, Federal Republic of Germany

Received 22 April 1993

Abstract. We investigate the dynamics of fracture of a surface layer which covers an elastically stretched substrate. For this we map the mechanical model onto its electrical counterpart, an array of resistors and fuses. We show the existence of an intrinsic correlation length which governs the process. Starting with the investigation of the failure characteristics of a single intact system, we obtain general expressions for the distribution of breakup currents and for the positions of failure; these allow us to describe the fragmentation process. We show that the distribution of fragment sizes and the mean fragment sizes often scale, and compare the analytical results to numerical simulations of the process.

1. Introduction

Numerous authors have paid attention to breaking phenomena in recent years [1–9]. Many papers have been devoted both to the geometry of single cracks and also to the statistical properties of an ensemble of cracks [1–9]. A special example is provided by the fragmentation of surface layers [10–12], with applications both in nature and technology. For example one can imagine the cracking of mud or paint upon drying or the rupture of coatings upon bending or stretching [13–15]. These systems share a distinctive property, namely the often large difference between the elastic properties of the bulk matter and those of the surface layer.

In the present article we analyse the statistics of fragmentation of surface layers. More specifically, we deal with problems that are one-dimensional by their physical nature, e.g. the breaking of a thin film covering a stretched sheet or a bent beam. In this case the stress field is taken to be homogeneous, and cracks grow perpendicular to the direction of the force. The latter condition is valid if the inhomogeneity in the constitution of the sample does not play a significant role. Our aim is to elucidate the interplay between the different parameters. We identify and describe different regimes, depending on the stage of fragmentation.

Of course, a one-dimensional model cannot account for such features as the shape of the cracks. Some of its properties, however, will also show up in more general two-dimensional systems. Among these will be the existence of a characteristic length scale describing the stress relaxation, and the presence of two different breaking regimes determined by whether the mean fragment size is larger or smaller than this characteristic length.

We analyse the probability at which a fragment of size N eventually breaks up at site k under a force F or, alternatively, in an electrical analogue, at a given current J. In the

† Also at: P N Lebedev Physical Institute of the Academy of Sciences of Russia, Leninsky Prospekt 53, Moscow 117924, Russia.

0305-4470/93/184521+17$07.50

limit of large N we obtain closed formulae for those breaking probabilities. This enables us to derive scaling laws connecting the average fragment size and the external stress or current. Numerical simulations are performed to verify the results.

The article is structured as follows. In section 2 we formulate our mechanical model and show that it is analogous to an electrical network. In section 3 we consider the properties of the electrical circuit and show that it displays a characteristic length scale. In section 4 we extensively consider the failure characteristics of a single fragment and present both analytical and numerical results. Section 5 is devoted to the analysis of the fragmentation process. In section 5.1 we consider the later stages of the fragmentation process and show that the distribution of fragment sizes exhibits scaling behaviour under a wide range of circumstances. In section 5.2 we deal with a different type of fragmentation process not discussed in section 5.1. Finally, in section 6 we present the conclusions and summarize the paper.

2. The model

The model we consider is the one-dimensional analogue of a construction used by Meakin [10–12], see figure 1(a). Imagine a bulk material covered by a brittle surface layer. Both the bulk and the surface layer are assumed to be chains of springs characterized by their elastic constants D and d, respectively. The surface is attached to the bulk elastically, so that the surface layer may move relatively to the bulk. This is described in our model by the nodes on the two chains being pairwise connected through leaf springs (of elastic constant δ). The surface layer is assumed to be brittle, so that each spring in it may break under stress. We denote the force at which the kth spring breaks by F_k.

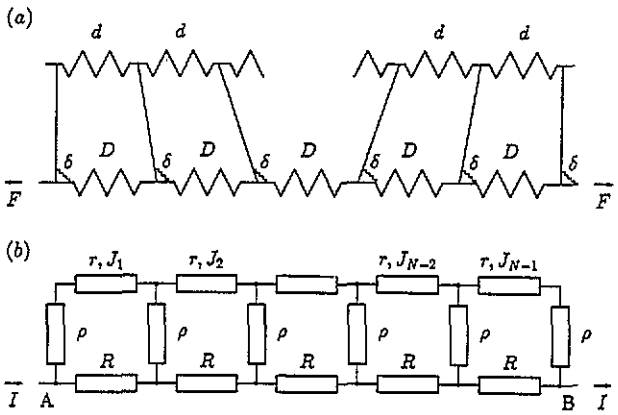

Figure 1. Mechanical (a) and electrical (b) realization of the one-sided ladder model; see text for details.

At small elongations the model is scalar; as we continue to show, it is then also analogous to the electrical circuit depicted in figure 1(b). The arguments which support the analogy are as follows. Mechanical forces at a point at rest cancel. Since we are only interested in motions parallel to the axis of the system, we neglect forces perpendicular to it. Then the electrical counterparts of the forces are currents; these satisfy Kirchhoff's current law, i.e. the sum of all currents entering a knot vanishes. Ohm's law $U = RI$ and Hooke's law

$x = D^{-1}F$ then imply that displacements in the mechanical model correspond to electrical voltage differences. In the same way the mechanical spring constants have the electrical conductivities R^{-1} as counterparts.

The arrangement shown in figure 1(b) is a one-sided ladder [17]; it differs from figure 1(a) only in that the R-resistors replace the D-springs; analogously, r replaces d and ρ replaces δ. The resistances are taken to be the same throughout each group of resistors; moreover, the r-resistors act as fuses as well. The currents J_k at which these fuses burn are then equivalent to the thresholds F_k in the mechanical model. We denote by $\varphi(J)$ the statistical distribution law which the J_ks obey. Furthermore, we assume $R \ll r$, so that the overall resistance of the ladder does not change by defecting fuses. This reflects the idea that—mechanically speaking—almost the entire strain energy is absorbed by the bulk material. Finally, the number of failed fuses will be taken to be small in comparison to the total number of fuses.

Our model parallels the random fuse model used by Duxbury *et al* [16], but in our case the model shows negative feedback, i.e. the formation of a new crack is less likely in the neighbourhood of a crack already present (vide infra).

In the following sections we discuss the model mostly in electrical terms.

3. Electrical properties of a single fragment

We consider a one-sided ladder of size N, consisting of $N-1$ elements; see figure 1(b). An external voltage is applied between A and B, causing an overall current I to flow. What is the value of the current j_k flowing through the kth fuse? Applying Kirchhoff's voltage law to the voltage differences around the kth circuit yields

$$0 = R(j_k - I) + \rho(j_k - j_{k-1}) + rj_k + \rho(j_k - j_{k+1}) \tag{1}$$

or

$$RI = j_k(R + 2\rho + r) - \rho(j_{k-1} + j_{k+1}). \tag{2}$$

This system of linear equations can be solved as in [17], where the calculations are performed in detail. Here we only sketch the main ideas.

The substitution $2\rho\cosh 2\mu = R + r + 2\rho$ or

$$\mu = 1/2\cosh^{-1}[1 + (R + r)/(2\rho)] \tag{3}$$

transforms equation (2) to

$$2j_k\cosh 2\mu = j_{k-1} + j_{k+1} + RI/\rho. \tag{4}$$

The general solution to this system of linear inhomogeneous equations is

$$j_k = (1 + \alpha e^{2k\mu} + \beta e^{-2k\mu})IR/(R + r) \tag{5}$$

as may be verified by insertion into equation (4). The j_ks satisfy the boundary conditions $j_0 = j_N = 0$. This determines the values of the coefficients α and β. One has

$$\alpha = -1/(1 + e^{2N\mu}) \tag{6}$$

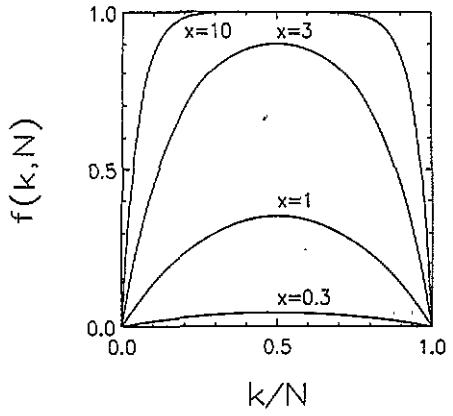

Figure 2. The current in a fragment $j_k/J = f(k, N)$ as given by equations (8) and (9). The values for $x = N\mu$ are 0.3, 1, 3, 10. Note the plateau region in the case $x = 10$.

and

$$\beta = -1/(1 + e^{-2N\mu}). \tag{7}$$

Now one can cast equation (5) into the compact form

$$j_k = f(k, N)J \tag{8}$$

with $J = IR/(R + r)$ and

$$f(k, N) = 1 - e^{2k\mu}/(1 + e^{2N\mu}) - e^{-2k\mu}/(1 + e^{-2N\mu}). \tag{9}$$

This function attains its maximum $f_{max} = 1 - 1/\cosh(N\mu)$ at $k_{max} = N/2$ and vanishes at $k = 0$ and $k = N$.

A plot of f as a function of k is given in figure 2 for some values of the parameter $x = N\mu$. From the plot two regimes are easily identified. For $N\mu \gg 1$ one has

$$f(k, N) = \begin{cases} 1 - e^{-2k\mu} & \text{for } k \ll N \\ 1 - e^{-2(N-k)\mu} & \text{for } N - k \ll N \\ 1 & \text{otherwise.} \end{cases} \tag{10}$$

We call the region for which $f(k, N) \approx 1$ holds the *plateau*. The plateau is clearly seen in figure 2 for $N\mu = 10$. Furthermore, the boundaries determine the regime outside the plateau; their region of influence is characterized by the *correlation length* $\xi \equiv 1/\mu$. The current through the fuses in the plateau region is simply given by J.

In the other limit $N\mu \ll 1$ one has by expanding the exponentials to second order

$$f(k, N) = \mu^2[N^2 - (N - 2k)^2]/2 = 2\mu^2 k(N - k) \tag{11}$$

f_{max} is then given by $f_{max} = \mu^2 N^2/2$.

For convenience we introduce the auxiliary function $g(\theta, x)$ according to

$$f(k, N) = f_{max} g(\theta, x). \tag{12}$$

Here $\theta = (k/N) - (1/2)$, $x = N\mu$, and g is given by

$$g(\theta, x) = \frac{\cosh(x) - \cosh(2x\theta)}{\cosh(x) - 1}. \tag{13}$$

Hence $g(\theta, x)$ is symmetrical in θ and ranges between 0 and 1 for $-1/2 \leqslant \theta \leqslant 1/2$. As $x \to \infty$, $g(\theta, x) \to 1$ for all $|\theta| < 1/2$, and for $x \ll 1$ one has

$$g(\theta, x) = g(\theta) = 1 - 4\theta^2 \tag{14}$$

independent of x.

4. Breaking characteristics of a single fragment

In this section we consider the failure of a fuse in an initially intact single fragment. The results (distributions of break-up currents and the position of the failing fuse) will turn out to be helpful in the analysis of the fragmentation process. Here we determine the break-up properties of a fragment using the distribution of fuse strengths.

4.1. General forms

We start from a fragment of the ladder of size N. We number the fuses of this fragment from 1 to $N-1$, and focus on the first fuse to burn.

For this we turn on and gradually increase J. All local currents j_k are proportional to J, so that we eventually reach a point where for the first time a fuse fails, i.e. is removed from the system *irreversibly*. Thus the corresponding current becomes $j'_k = 0$, where the prime denotes the situation after the failure, and k is the number of the corresponding fuse. The set of currents j'_m for the newly formed fragments of sizes k and $N-k$, respectively, follows from equations (8) and (9):

$$j'_m = \begin{cases} f(m,k)J & \text{for } 0 \leqslant m \leqslant k \\ f(m-k, N-k)J & \text{for } k+1 \leqslant m \leqslant N. \end{cases} \tag{15}$$

Here we use the fact that $R \ll r$, so that the overall current is not affected by the failure of the fuse.

Let us now compute the probability that the kth fuse is the first one to fail. Given J, the probability density $\psi_k(J)\,\mathrm{d}J$ for the fuse k to fail is

$$\psi_k(J)\,\mathrm{d}J = \varphi[f(k,N)J]f(k,N)\,\mathrm{d}J \tag{16}$$

where we use the fact that the distribution of maximal currents is $\varphi(i)$.

We now introduce the distribution function $F(i) = \int_0^i \varphi(i')\,\mathrm{d}i'$. The probability that the kth fuse does not fail when the external current is increased up to J is given by $1 - \int_0^J \psi_k(\tilde{J})\,\mathrm{d}\tilde{J} = 1 - F[f(k,N)J]$. Then the joint probability density $p_N(k,J)$ for the kth fuse to fail when the current reaches the value J while all other fuses stay intact is given by

$$p_N(k,J) = f(k,N)\varphi[f(k,N)J] \prod_{m \neq k} [1 - F(f(m,N)J)] \tag{17}$$

or, equivalently, by

$$p_N(k,J) = \frac{f(k,N)\varphi[f(k,N)J]}{1 - F(f(k,N)J)} \exp\left(\sum_{m=0}^{N} \ln[1 - F(f(m,N)J)] \right). \tag{18}$$

The integration of equation (18) with respect to J yields the total probability $q(k|N)$ for a fragment of size N to break at the position k:

$$q(k|N) = \int_0^\infty p_N(k,J)\,\mathrm{d}J. \tag{19}$$

From equation (18) one can readily infer that the $q(k|N)$ are normalized, i.e. that

$$\sum_{k=1}^{N} q(k|N) = 1 \tag{20}$$

holds. To see this one only has to notice that the prefactors of the exponentials are the derivatives of the corresponding exponents with regard to J, see equation (16) and the definition of F. Similarly, the summation with respect to k gives the distribution $r(J|N)$ of the break-up currents:

$$r(J|N) = \sum_{k=0}^{N} p_N(k, J). \tag{21}$$

A more convenient form of equation (18) holds for N large. In this case we can revert from the summation to an integration over m. This corresponds to viewing m (or, equivalently, k) as being continuous. We hence change from k to θ, from m to β, furthermore, according to equation (12), from $f(k, N)$ to $g(\theta, x)$, from J to $y = Jf_{\max}$, and from $p_N(k, J)$ to $P_N(\theta, y) = Nf_{\max}p_N(k, J)$. We obtain

$$P_N(\theta, y) = N\frac{g(\theta, x)\varphi[g(\theta, x)y]}{1 - F(g(\theta, x)y)} \exp\left(N\int_{-1/2}^{1/2} \ln[1 - F(g(\beta, x)y)]\,\mathrm{d}\beta\right). \tag{22}$$

This is the expression we looked for.

Now our task is to evaluate equation (22) for different x and for different types of densities φ. A simple case holds for $x \gg 1$. This case is characterized by the appearance of a plateau regime. Here $g(\theta, x) \simeq 1$, independent of θ. Now one can (by neglecting the influence of the small regions at the boundaries) evaluate equation (22) in a straightforward manner:

$$P_N(\theta, y) \simeq N\frac{\varphi(y)}{1 - F(y)} \exp(N \ln[1 - F(y)]) = -\frac{\mathrm{d}}{\mathrm{d}y}[1 - F(y)]^N \tag{23}$$

an expression independent of θ. Evidently, in the plateau regime breaks are homogeneously distributed in space.

The other limit is $x \ll 1$, for which $f_{\max} = x^2/2$, and $g(\theta, x) = 1 - 4\theta^2$ is parabolic and independent of x, see equation (14). Denoting by $\Phi(y|N)$ the exponential expression in equation (22)

$$\begin{aligned}\Phi(y|N) &= \exp\left(N\int_{-1/2}^{1/2} \ln[1 - F(g(\beta, x)y)]\,\mathrm{d}\beta\right) \\ &= \exp\left(N\int_{-1/2}^{1/2} \ln[1 - F(y - 4\beta^2 y)]\,\mathrm{d}\beta\right)\end{aligned} \tag{24}$$

the probability density for the fuse at the coordinate θ to fail is

$$Q(\theta|N) = N\int_0^\infty \frac{(1 - 4\theta^2)\varphi(y - 4\theta^2 y)}{1 - F(y - 4\theta^2 y)}\Phi(y|N)\,\mathrm{d}y. \tag{25}$$

Furthermore, the probability density for the current $y = Jf_{\max}$ to induce a failure is

$$R(y|N) = N\int_{-1/2}^{1/2} \frac{(1 - 4\theta^2)\varphi(y - 4\theta^2 y)}{1 - F(y - 4\theta^2 y)}\Phi(y|N)\,\mathrm{d}\theta = -\frac{\mathrm{d}\Phi(y|N)}{\mathrm{d}y}. \tag{26}$$

We furthermore note that the integrand in equation (24) is negative. For large N the following approximation is justified:

$$\Phi(y|N) \simeq \exp\left(-2N\int_0^{1/2} F(y - 4\beta^2 y)\,\mathrm{d}\beta\right). \tag{27}$$

The reason is that $F(y - 4\beta^2 y)$ is either relatively small for all values of β, which allows the logarithm to be expanded to lowest order or that it is large in a certain β-interval, in which case Φ is practically zero anyhow.

4.2. Rectangular φ-distributions

As examples, we take rectangular forms for the probability distributions $\varphi(i)$ at which the fuses fail [20]

$$\varphi(i) = \begin{cases} 1/W & \text{for } i_{\min} \leqslant i < i_{\min} + W \\ 0 & \text{otherwise.} \end{cases} \tag{28}$$

In these cases we have

$$F(i) = \begin{cases} 0 & \text{for } i < i_{\min} \\ (i - i_{\min})/W & \text{for } i_{\min} \leqslant i < i_{\min} + W \\ 1 & \text{for } i \geqslant i_{\min} + W. \end{cases} \tag{29}$$

Now the integration in equation (27) for $x \ll 1$ can be performed explicitly. Evidently, for $y < i_{\min}$ one has $\Phi(y|N) = 1$, whereas for $y > i_{\min}$ we find

$$\Phi(y|N) \simeq \exp\left(-\frac{2N(y - i_{\min})^{3/2}}{3W\sqrt{y}}\right). \tag{30}$$

Using this expression $Q(\theta|N)$, equation (25), and $R(y|N)$, equation (26), can be computed. The results depend on whether $i_{\min} = 0$ or $i_{\min} > 0$. For $i_{\min} > 0$ we may replace in equation (30) y by $i_{\min}$ in the denominator and once more take $F(y - 4\beta^2 y)$ in the denominator of equation (25) to be small. We obtain for Q in this approximation

$$Q(\theta|N) = \frac{1}{2\Delta}\Gamma\left[\frac{2}{3}, \left(\frac{|\theta|}{\Delta}\right)^3\right]. \tag{31}$$

In equation (31) $\Gamma(\alpha, x)$ denotes the incomplete Γ-function and $\Delta = (3W/(16 i_{\min} N))^{1/3}$. We note that $Q(\theta|N)$ is now a bell-shaped function of width Δ and is concentrated in the middle of the segment. We have verified numerically that equation (31) is quite accurate in the range $0 < \Delta < 1/3$. Hence for $i_{\min} > 0$ the fuses in the middle of the segment are most affected by failures; the effect is much stronger than the distribution of currents would suggest.

For $i_{\min} = 0$ equation (30) simplifies to

$$\Phi(y|N) \simeq \exp\left(-\frac{2N}{3W}y\right). \tag{32}$$

One obtains from equation (25)

$$Q(\theta|N) = (3/2)(1 - 4\theta^2). \tag{33}$$

Now the failures follow the distribution of currents closely. Note also that for $i_{\min} = 0$ the distribution $Q(\theta|N)$ is independent of N, whereas for $i_{\min} > 0$ its width is N-dependent, so that for large N it is strongly concentrated near $\theta = 0$. Therefore for $i_{\min} > 0$ the fragmentation process is almost regular, provided that $x \ll 1$. Thus the cases $i_{\min} = 0$ and $i_{\min} > 0$ give rise to quite different types of fragmentation.

In the case $i_{\min} > 0$ the probability distribution $R(y|N)$ of the current at which the first fuse of the considered segment fails follows from equations (26) and (24):

$$R(y|N) = \frac{N}{W}\sqrt{\frac{y - i_{\min}}{i_{\min}}}\exp\left(-\frac{2N(y - i_{\min})^{3/2}}{3W\sqrt{i_{\min}}}\right) \tag{34}$$

for $y > i_{\min}$, and $R(y|N) = 0$, otherwise. Note that the distribution $R(y|N)$ is concentrated near $y = i_{\min}$.

In a similar way from equations (24) and (32) we find for $i_{\min} = 0$

$$R(y|N) = \frac{2N}{3W} \exp\left(-\frac{2N}{3W} y\right) \tag{35}$$

for $y \geqslant 0$.

4.3. General φ-distributions

We now consider more general $\varphi(i)$-distributions, as described by the following form:

$$\varphi(i) = \begin{cases} 0 & \text{for } i < i_{\min} \\ A(\alpha+1)(i - i_{\min})^{\alpha} & \text{for } i_{\min} \leqslant i \leqslant i_{\min} + W \\ 0 & \text{for } i > i_{\min} + W. \end{cases} \tag{36}$$

Here α, A and W are parameters, and we restrict ourselves to $\alpha > -1$. For these distributions the $F(i)$ read

$$F(i) = \begin{cases} 0 & \text{for } i < i_{\min} \\ A(i - i_{\min})^{\alpha+1} & \text{for } i_{\min} \leqslant i \leqslant i_{\min} + W \\ 1 & \text{for } i > i_{\min} + W \end{cases} \tag{37}$$

where $A = W^{-1/(\alpha+1)}$.

Inserting equation (37) into equation (27) gives, for $x \ll 1$,

$$\Phi(y|N) \simeq \begin{cases} 1 & \text{for } y < i_{\min} \\ \exp(-N I_\alpha A (y - i_{\min})^{\alpha+3/2}/\sqrt{y}) & \text{for } y \geqslant i_{\min}. \end{cases} \tag{38}$$

Here I_α is given by

$$I_\alpha = 2\int_0^{1/2} (1 - 4\beta^2)^{\alpha+1}\, d\beta = \frac{\sqrt{\pi}}{2} \frac{\Gamma(\alpha+2)}{\Gamma(\alpha+5/2)} \tag{39}$$

with Γ being the ordinary Γ-function.

The case $i_{\min} > 0$ is similar to what is found for a rectangular distribution, equation (28). Replacing y by $i_{\min}$ in the denominator of equation (38), replacing $(1 - 4\theta^2)^{-1}$ by $1 + 4\theta^2$, and neglecting $F(y - 4\beta^2 y)$ in the denominator of equation (25), we obtain an infinite series:

$$Q(\theta|N) = \frac{\alpha+1}{2\alpha+3} \frac{1}{I_\alpha \Delta} \sum_{k=0}^{\infty} \binom{\alpha}{k} (-1)^k \left(\frac{|\theta|}{\Delta}\right)^{2k} \Gamma\left(\frac{2\alpha+2-2k}{2\alpha+3}, \left(\frac{|\theta|}{\Delta}\right)^{2\alpha+3}\right). \tag{40}$$

with $\Delta = (N I_\alpha A i_{\min}^{\alpha+1})^{-1/(2\alpha+3)}/2$, and where the binomial coefficients are, as usual,

$$\binom{\alpha}{k} = \frac{\Gamma(\alpha+1)}{\Gamma(k+1)\Gamma(\alpha-k+1)}. \tag{41}$$

The series simplifies to equation (31) in the case $\alpha = 0$, and truncates after $\alpha + 1$ terms if α is an integer. Similarly to the case $\alpha = 0$, it is a bell-shaped function of width Δ, concentrated at the middle of the segment.

Concerning the distribution of burning currents, for $i_{\min} > 0$ equations (27) and (38) imply

$$R(y|N) \simeq \frac{NI_\alpha A}{\sqrt{i_{\min}}}\left(\alpha+\frac{3}{2}\right)(y-i_{\min})^{\alpha+1/2}\exp\left(-\frac{NI_\alpha A}{\sqrt{i_{\min}}}(y-i_{\min})^{\alpha+3/2}\right) \tag{42}$$

$$\simeq \frac{1}{\tau}\left(\alpha+\frac{3}{2}\right)\left(\frac{y-i_{\min}}{\tau}\right)^{\alpha+1/2}\exp\left(-\left[\frac{y-i_{\min}}{\tau}\right]^{\alpha+3/2}\right) \tag{43}$$

provided that $y \geqslant i_{\min}$. If $y < i_{\min}$, we have $R(y|N) = 0$. Here τ is given by $(NI_\alpha A i_{\min}^{-1/2})^{-2/(2\alpha+3)}$.

The results equations (40) and (43) have been checked by numerical simulations. The distributions Q and R have been obtained through 10^4 realizations in which a ladder of size $N = 100$ was broken into two pieces. The parameters of the distributions used are $i_{\min} = 1$, $A = 1$ and $W = 1$, see equation (36). Figures 3(a), (b), and (c) correspond to the values of $\alpha = 0$, 1 and 2, respectively, see section 4.2. In figure 3 the relative positions θ and relative currents y at which the first fuses fail are given in units of their characteristic values Δ and τ. Note the fair coincidence between the analytical forms and the results of the simulations. Note also the fact that $\Delta \sim N^{-1/(2\alpha+3)}$ and $\tau \sim N^{-2/(2\alpha+3)}$ are very small for large fragment sizes.

In the case $i_{\min} = 0$ equation (38) simplifies to

$$\Phi(y|N) \simeq \exp(-NI_\alpha A y^{\alpha+1}) \tag{44}$$

and equation (25) yields

$$Q(\theta|N) \simeq (1-4\theta^2)^{\alpha+1}/I_\alpha. \tag{45}$$

We also obtain

$$R(y|N) \simeq \frac{1}{\omega}(\alpha+1)\left(\frac{y}{\omega}\right)^{\alpha}\exp\left(-\left[\frac{y}{\omega}\right]^{\alpha+1}\right) \tag{46}$$

with $\omega = (NI_\alpha A)^{-1/(\alpha+1)}$.

The results of the numerical simulations are displayed in figure 4, together with the analytical forms, equations (45) and (46). All parameters (apart from $i_{\min}$) are the same as in figure 3.

Note that in this case the width of the Q-distribution does not depend on the size of the ladder and thus remains finite in the limit of large N. Thus we expect the resulting fragmentation process to differ significantly from the one obtained under the condition $i_{\min} > 0$, vide infra.

We see that in both cases only the behaviour of $\varphi(i)$ in a small neighbourhood of $i = i_{\min}$ enters the analysis. Therefore distributions $\varphi(i)$ admitting a low-end expansion according to equation (36) lead to the same probability distributions R and Q as those given by equations (40), (45), (43) and (46). Thus the type of fragmentation behaviour is determined solely by the values of $i_{\min}$ and α, but not by the behaviour of $\varphi(i)$ at larger values of i, a result which we have also verified numerically.

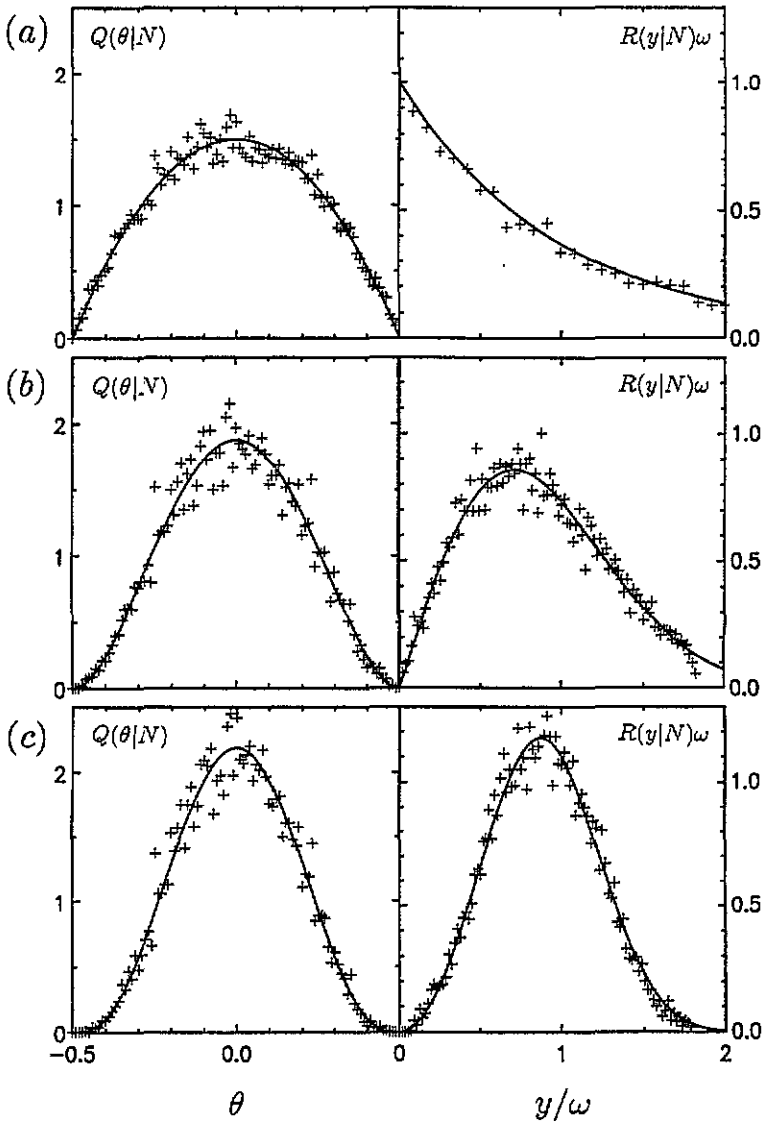

Figure 3. The distributions $Q(\theta|N)$ and $R(y|N)$ in the case $i_{\min} > 0$ (see text for details). Note the different scales. The full curves correspond to the analytical forms, equations (40) and (43); crosses represent the simulation results. In cases (a), (b) and (c) α is 0, 1, and 2, respectively.

5. The fragmentation process

After establishing the probability distributions for the first fracture of a single chain, we now investigate the successive breaking of an initially intact system into several pieces. First we focus on the dependence of the average fragment size $\langle L \rangle$ on J. At the beginning of the process, if $\langle L \rangle \gg \xi$, new fractures form independently of each other and mostly in plateau regions. The number of fractures is proportional to $F(J)$, with $F(J)$ being the cumulative distribution function of φ. As the process continues, one eventually enters the regime characterized by $\langle L \rangle \lesssim \xi$. We now consider this later stage.

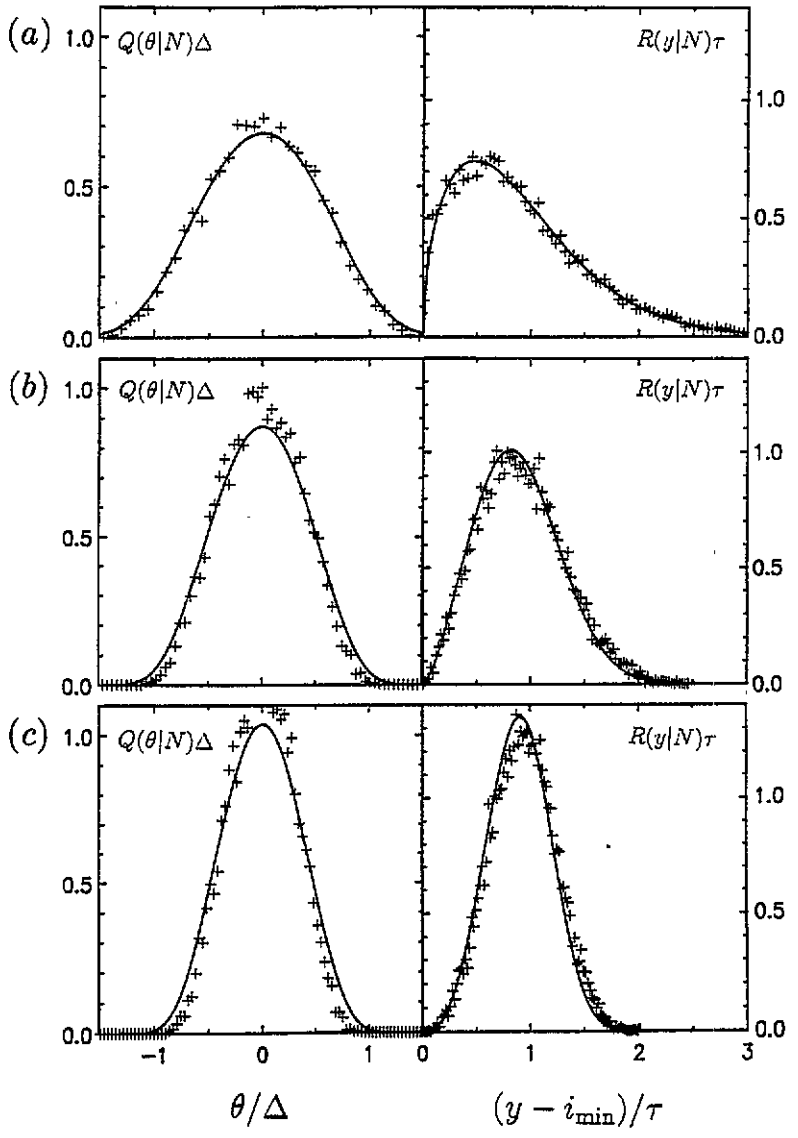

Figure 4. The same as in figure 3, now for $i_{\min} = 0$. The full curves correspond to the analytical forms, equations (45) and (46). In cases (a), (b) and (c) α is 0, 1, and 2, respectively. Note the change of units from figure 3.

First we present the results of the numerical simulations (see [20] for a description of the algorithm). Figures 5(a) to (d) present the dependence of $\langle L \rangle$ on J, plotted in a double-logarithmical scale. The simulations were done on a system whose total number of fuses N_0 equals 5×10^5. Furthermore, the inverse correlation length μ was chosen to be 0.001 66 in (a), 10^{-6} in (c) and in (d). In case (a) the rectangular distribution $\varphi(i) = 1/2$ for $0 \leqslant i \leqslant 2$ was used, in (c) the form $\varphi(i) = 2i$ for $0 \leqslant i \leqslant 1$, and in (d) the form $\varphi(i) = 3i^2$ for $0 \leqslant i \leqslant 1$. Since, according to the previous section, α is given by the order with which φ vanishes at $i = 0$, these cases stand for $\alpha = 0$, 1 and 2, respectively. figure 5(d) corresponds to a ladder of length $N_0 = 5 \times 10^5$ and inverse correlation length

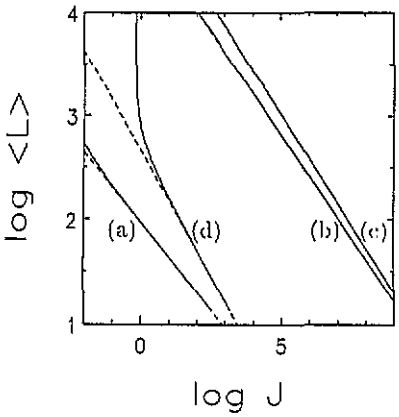

Figure 5. The dependence of the mean fragment size on the external voltage for different distributions φ. In cases (a), (c) and (d) α is 0, 1, and 2. Here $i_{min} = 0$. Case (b) corresponds to a rectangular distribution with $i_{min} > 0$. See text for details.

$\mu = 0.001\,66$. Here $\varphi(i)$ is rectangular, with $i_{min} = 0.7$ and $W = 0.6$, see equation (28).

We see that at the later stages of the fragmentation process the dependence of $\langle L \rangle$ on J is given by a power law

$$\langle L \rangle \sim J^{\beta} \tag{47}$$

where the exponent β depends on the distribution $\varphi(i)$. The numerical values of the exponents obtained correspond to $\beta = -0.335$ in (a), $\beta = -0.394$ in (c), $\beta = -0.420$ in (d), and $\beta = -0.493$ for the distribution with $i_{min} > 0$, case (b). The numerical accuracy of all values is ± 0.005.

We also see that the overall behaviour of the process is somewhat different in the cases $i_{min} = 0$ and $i_{min} > 0$. In the following two subsections we will analyse the process form a theoretical point of view and obtain

$$\beta = -\frac{\alpha + 1}{2\alpha + 3} \tag{48}$$

in the case $i_{min} = 0$ and

$$\beta = -\tfrac{1}{2} \tag{49}$$

for $i_{min} > 0$, i.e. we infer the values $\beta = -0.333$, -0.4, -0.428 and -0.5 for (a) to (d), respectively. As already shown, our simulations agree very well with these results.

5.1. Scaling fragmentation

We first analyse the case $i_{min} = 0$. We will restrict ourselves to situations where the number of fuses that fail is small compared to the total number of fuses. Therefore changes in φ may be ignored.

With this approximation the fragmentation process can be described by the kinetic equation [18, 19]

$$\frac{\partial n(L, J)}{\partial J} = -r(J|L)n(L, J) + 2\int_{L}^{\infty} n(L', J)p_{L'}(L, J)\,\mathrm{d}L' \tag{50}$$

with $n(L, J)$ being the fragment size distribution at a given J. The meaning of the two terms on the right-hand side of equation (50) is evident: the first one describes the decrease

in the number of fragments of size L due to splitting (with probability density $r(J|L)$ and L taken to be a continuous variable), and the second term reflects the creation of new fragments of size L by the splitting of larger fragments of size L'. The factor of two stems from the fact that this event can take place with equal probability either at position L or at $L'-L$. Furthermore, $r(J|L)$ and $p_{L'}(L, J)$ are defined as in the previous chapter. Neglecting the denominator in equation (18) their explict forms are

$$p_{L'}(L, J) = A(\alpha+1)\left(\frac{\mu^2}{2}\right)^{\alpha+1} \times \left(g\left(\frac{L}{L'}-\frac{1}{2}, 0\right)\right)^{\alpha+1} L^{\prime 2\alpha+2} J^{\alpha} \exp\left(-\left(\frac{\mu^2}{2}\right)^{\alpha+1} A I_\alpha L^{\prime 2\alpha+3} J^{\alpha+1}\right) \quad (51)$$

and

$$r(J|L) = A(\alpha+1)(\tfrac{1}{2}\mu^2)^{\alpha+1} I_\alpha L^{2\alpha+3} J^{\alpha} \exp(-(\tfrac{1}{2}\mu^2)^{\alpha+1} A I_\alpha L^{2\alpha+3} J^{\alpha+1}). \quad (52)$$

Let us now look for a scaling solution of equation (50) of the form

$$n(L, J) = \frac{1}{L_c}\rho\left(\frac{L}{L_c}\right) \quad (53)$$

which depends on J only through the characteristic length scale $L_c(J)$; $\rho(\eta)$ is then a universal function of the (dimensionless) length variable $\eta = L/L_c$. The value L_c must be chosen in such a way that the substitution of equation (50) into equation (53) yields a dimensionless differential equation for $\rho(\eta)$. This leads us to the choice

$$L_c = \left[\left(\frac{\mu^2}{2}\right)^{\alpha+1} A I_\alpha J^{\alpha+1}\right]^{-1/(2\alpha+3)}. \quad (54)$$

L_c is unique up to a proportionality constant.

From equation (53) we immediately obtain

$$\langle L\rangle = L_c \int_0^\infty \eta\rho(\eta)\,\mathrm{d}\eta. \quad (55)$$

We therefore expect $\langle L\rangle$ to scale according to

$$\langle L\rangle \sim L_c \sim J^{-(\alpha+1)/(2\alpha+3)} \quad (56)$$

in agreement with our numerical simulations, see figures 5(a) to (c).

We can now show the existence of scaling solutions by plotting, at different stages of the fragmentation process, the ensuing distributions as functions of the normalized fragment length $L/\langle L\rangle$. The results of simulations for three different distributions are presented in figures 6(a) to (c). Parallelling figure 5, case (a) corresponds to $\varphi(i) = 1/2$ for $0 \leqslant i \leqslant 2$, (b) to $\varphi(i) = 2i$ for $0 \leqslant i \leqslant 1$, and (c) to $\varphi(i) = 3i^2$ for $0 \leqslant i \leqslant 1$. Thus α is once more given by 0, 1 and 2, respectively. N_0 equals 2×10^6 in case (a), 5×10^5 otherwise, and μ equals 10^{-6} in all cases. The crosses, triangles, squares and circles correspond to $\langle L\rangle = 1000$, 204, 68 and 20 in figure 6(a), 545, 136, 45 and 14 in figures 6(b) and (c), respectively. Note that the forms of the distributions are independent of the stage of the fragmentation process; this is a strong support for our scaling hypothesis, equation (53), as $\langle L\rangle$ is proportional to L_c, see equation (55).

We now turn to the case $i_{\min} > 0$, which gives rise to a different type of fragmentation process.

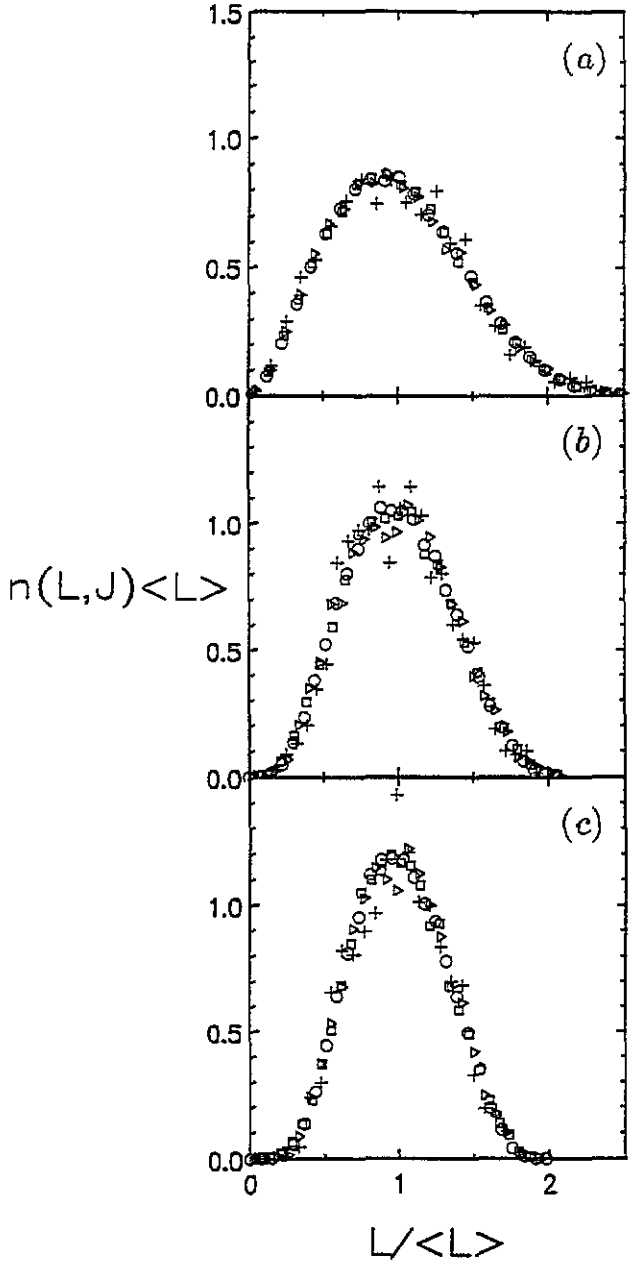

Figure 6. The distributions of fragment sizes, plotted as functions of $L/\langle L\rangle$. In cases (a), (b) and (c) α is 0, 1 and 2, respectively. The crosses, triangles, squares and circles display the results for different stages of the process. See text for details.

5.2. Hierarchical fragmentation

In the case $i_{\min} > 0$ the later stages of the process are characterized by narrow distributions of θ and y, see equation (38). If $\langle L\rangle < \xi$, the fragments therefore break up close to their middle, where the current attains its maximum. This gives rise to a hierarchical series of

fractures, as we show in this section.

Let us assume that upon entering the hierarchical regime, we have a fragment size distribution $n_0(L)$. The maximum current flows in the middle of the largest segment, which therefore breaks up next as the process continues. It produces two new segments of nearly equal sizes. We thus find a characteristic length L_c defined as the size of the fragment which is about to break (i.e. the presently largest fragment). The value of L_c is determined by the fact that this fragment breaks at $y = i_{min}$ or $J = 2i_{min}/(\mu L_c)^2$. Therefore L_c is given by

$$L_c = \frac{1}{\mu}\sqrt{\frac{2i_{min}}{J}}. \tag{57}$$

We now freeze the process at a given stage defined by L_c and denote the resulting distribution by $n(L, L_c)$. Both n and n_0 are normalized to unity. For simplicity we assume in the following analysis that breaks occur exactly at the centre of the fragments.

Then new fragments of size less than $L_c/2$ could not be yet formed, so for $L < L_c/2$ $n(L, L_c)$ is equal to $n_0(L)$ up to a constant due to normalization. Second, by assumption, no fragments larger than L_c have survived, so for $L > L_c$ we have $n(L, L_c) = 0$.

Let us now pick $L \in (L_c/2, L_c)$. The number of fragments $n(L, L_c)\,dL$ of sizes between L and $L + dL$ now is given by those fragments that were present initially, $n_0(L)\,dL$, plus the two halves of the original fragments of length $2L$ having undergone one fracture, $2n_0(2L)\,d(2L)$, plus the four quarters of the original fragments of length $4L$ having undergone two fractures, $4n_0(4L)\,d(4L)$, etc. Thus

$$n(L, L_c)\,dL \sim \sum_{k=0}^{\infty} 2^k n_0(2^k L)\,d(2^k L) \tag{58}$$

$$\sim \sum_{k=0}^{\infty} 4^k n_0(2^k L)\,dL \qquad \text{for } L \in (L_c/2, L_c). \tag{59}$$

By introducing the normalization constant A we obtain

$$n(L, L_c) = \begin{cases} \dfrac{n_0(L)}{A} & \text{for } L \leqslant L_c/2 \\ A^{-1} \displaystyle\sum_{k=0}^{\infty} 4^k n_0(2^k L) & \text{for } L_c/2 < L \leqslant L_c \\ 0 & \text{for } L > L_c. \end{cases} \tag{60}$$

The normalization constant A is determined by

$$A = \int_0^{L_c/2} n_0(\xi)\,d\xi + \sum_{k=0}^{\infty} 2^k \int_{2^{k-1}L_c}^{2^k L_c} n_0(\xi)\,d\xi \tag{61}$$

A grows rapidly as L_c decreases, and therefore the distribution $n(L, L_c)$ as given by equation (60) also vanishes for $L < L_c/2$. Thus at the later stages of the process fragments have sizes L satisfying $L_c/2 \leqslant L \lesssim L_c$, and

$$\langle L \rangle = \kappa L_c \tag{62}$$

with $1/2 < \kappa < 1$. According to equations (57) and (62) one then has

$$\langle L \rangle \sim J^{-1/2} \tag{63}$$

independently of the precise form of φ. The distribution of fragment sizes $n(L, L_c)$ is nonetheless non-universal, i.e. it depends explicitly on $\varphi(i)$ and $n_0(L)$.

Note that the onset of the fragmentation process is different from the cases considered in the previous subsection. The first failures occur at $J = i_{\min}$ or, in our case, at $\log(J) = \log 0.7 = -0.155$, see figure 5(d). In the doubly logarithmical representation, at higher currents the slope of $\log\langle L \rangle$ approaches $-1/2$ to a good accuracy.

6. Summary

In this work we have introduced a model for the fracture of surface layers, and have also presented its electrical analogue, a ladder of resistors with fuses sitting on one side. As we have shown, the model displays two different regimes for the fragmentation process, depending on whether the mean fragment size is large or small compared to an intrinsic correlation length. Starting from the failure characteristics of an intact segment we have established analytically the main features of a series of fragmentation steps. We have confirmed the results—the distributions of the positions of failure and the distributions of the break-up currents—through numerical simulations. Furthermore, we have shown that after an initial stage of the process the mean fragment size $\langle L \rangle$ decreases according to a power law, $\langle L \rangle \sim J^{\beta}$, as a function of the externally applied force or current, J. Here the exponent β depends on the form of φ near the origin. If $\varphi(i) \sim i^{\alpha}$ for small i, we obtain $\beta = -(\alpha+1)/(2\alpha+3)$. The resulting distributions of fragment sizes also scale accordingly. On the other hand, if $\varphi(i) = 0$ for $0 \leqslant i \leqslant i_{\min}$, we have $\beta = -1/2$. All these analytically obtained results were confirmed through numerical simulations.

Acknowledgments

The authors are indebted to P Alemany, Dr L de Arcangelis, Professor T L Chelidze, Dr H J Herrmann, S Luding and Dr U Zürcher, for helpful discussions. Support by the Fonds der Chemischen Industrie, by the Deutsche Forschungsgemeinschaft (SFB 60), and by the NATO research grant RG 0115/89 is gratefully acknowledged.

References

[1] de Arcangelis L, Redner S and Herrmann H J 1985 *J. Physique* **13** L585
[2] de Arcangelis L and Herrmann H J 1989 *Phys. Rev.* B **39** 2678
[3] de Arcangelis L, Hansen A, Herrmann H J and Roux S 1989 *Phys. Rev.* B **40** 877
[4] Herrmann H J, Hansen A and Roux S 1989 *Phys. Rev.* B **39** 637
[5] Herrmann H J and de Arcangelis L 1989 *Disorder and Fracture (NATO ASI Series 234)* ed J C Charmet, S Roux and E Guyon (New York: Plenum) p 149
[6] Herrmann H J 1991 *Phys. Scr.* T **38** 13
[7] Kahng B, Batrouni G G, Redner S, de Arcangelis L and Herrmann H J 1988 *Phys. Rev.* B **37** 7625
[8] Taguchi Y h 1989 *Physica* A **156** 741
[9] Roux S, Hansen A, Hinrichsen E L and Sornette D 1991 *J. Phys. A: Math. Gen.* **24** 1625
[10] Meakin P 1987 *Thin Solid Films* **151** 165

[11] Meakin P, Li G, Sander L M, Yan H *et al* 1989 *Disorder and Fracture (NATO ASI Series 234)* ed J C Charmet, S Roux E and Guyon (New York: Plenum) p 119
[12] Meakin P 1990 *Statistical Models for the Fracture of Disordered Media* ed H J Herrmann and S Roux (Amsterdam: North-Holland–Elsevie) p 291
[13] Järvinen R, Mäntyla T and Kettunen P 1984 *Thin Solid Films* **114** 311
[14] Pellicori S F 1984 *Thin Solid Films* **113** 287
[15] Phillips J M, Feldman L C, Gibson J M and McDonald M L 1983 *Thin Solid Films* **107** 217
[16] Duxbury P M and Li Y 1989 *Disorder and Fracture (NATO ASI Series 234)* ed J C Charmet, S Roux and E Guyon (New York: Plenum) p 141
[17] Clerc J P, Giraud G, Laugier J M and Luck J M 1990 *Adv. Phys.* **39** 191
[18] Redner S 1989 *Disorder and Fracture (NATO ASI Series 234)* ed J C Charmet, S Roux and E Guyon (New York: Plenum) p 31
[19] Redner S 1990 *Statistical Models for the Fracture of Disordered Media* ed H J Herrmann and S Roux (Amsterdam: North-Holland–Elsevier) p 321
[20] Morgenstern O, Sokolov I M and Blumen A 1993 *Europhys. Lett.* **22** 487